

Novel Electrode Configuration for Ionic Wind Generation in Air at Atmospheric Pressure

Dorian Colas, Antoine Ferret, Ignazio Sciacca, David Z. Pai, Deanna A. Lacoste, Christophe O. Laux
*Laboratoire EM2C, CNRS UPR 288, École Centrale Paris,
Grande Voie des Vignes, 92290 Châtenay-Malabry, France*

Abstract

A novel electrode configuration is presented to generate ionic wind with a DC corona discharge in air at atmospheric pressure. The objective of the work is to maximize the power supplied to the flow in order to increase acceleration while avoiding breakdown. Thus, the proposed experimental setup addresses the problem of de-coupling the mechanism of ion generation from that of ion acceleration. Using a wire-plate configuration as a reference, we have focused on improving the topography of the electric field to 1) create separate ionization and acceleration zones in space, and 2) guide the trajectory of charged particles as parallel to the median axis as possible. In the new wire-cylinder-plate setup, a DC corona discharge is generated in the space between a wire and two cylinders. The ions produced by the corona then drift past the cylinders and into a channel between two plates, where they undergo acceleration. To maximize the ionic wind it is found that the geometric configuration must be as compact as possible and that the voltage applied must be right below breakdown. Experimentally, the optimized reference setup and the new configuration provide flow velocities up to 8 and 10 m/s, respectively, as well as a flow rate and thrust per unit electrode length up to 0.17 and 0.2 m²/s and 4.5 and 6.5 N/m, respectively. In comparison with a wire-wire corona configuration, the experimental results show that the ionic wind speed is increased by up to a factor of 2.

1. Introduction

The effect of the ionic wind created by a corona discharge or a dielectric barrier discharge on the boundary layer of an airfoil has interesting potential applications for the purpose of reducing drag, increasing lift during takeoff and landing, controlling the transition to turbulence, and for flow actuation. Forte *et al.*[1], Corke *et al.*[2] and Opaitis *et al.*[3] showed that the ionic wind can be used to sustain the boundary layer of a low-speed flow using surface discharges produced by Dielectric Barrier Discharges (DBD). Although the velocities produced are not yet elevated enough for applications to high-speed flows, progress has been made in increasing the induced flow speed produced by DBDs up to 6-7 m.s⁻¹ and in understanding the ionic wind phenomenon through modeling (Corke *et al.* [4], Moreau *et al.* [5], Boeuf *et al.* [6], Matteo-Velez *et al.*[7], Berard *et al.*[8]).

We examine here an alternate configuration using a corona discharge. The principle of the ionic wind produced by a corona between two cylindrical wires can be explained as follows (Lacoste *et al.* [9]). Around each wire, the electric field decreases inversely proportional to the distance to the wire. For small wire diameters, the electric field in the vicinity of the wire brought to a high potential is sufficient to ionize air. The positive ions generated at the anode drift toward the cathode while the negative ions stay close to the anode. In their movement, the positive ions transfer momentum to the neutral molecules via collisions. At the vicinity of the cathode, electrons attach to oxygen and O₂⁻ drifts toward the anode, transferring momentum to the neutrals. Two opposite charge currents appear. The net flow is called the ionic wind. When the electrodes are asymmetric (e.g. small diameter anode and large diameter cathode), the positive ion current dominates and the effect of the ionic wind is maximum.

Two types of DC corona discharges have been previously used for ionic wind generation. The first type is a DC surface corona discharge produced between two wires placed on the surface of an airfoil. This setup has been studied by Moreau *et al.* [5] under various aerodynamic conditions and has proven to generate speed flows up to 5 m.s⁻¹. As for the DBD surface discharges, maximum values of the thrust per unit electrode length generated by the ionic wind are about 80 mN/m.

The second type is a DC corona discharge between two free-standing wire electrodes in air. This setup has been studied by Berard *et al.* [6], who showed that flow velocities up to 3.5 m.s⁻¹ could be generated. Because acceleration and ionization are coupled, higher velocities could not be attained as the power supplied to the fluid was limited by the apparition of a spark.

The present investigation extends the work of Berard *et al.* [8] and Lacoste *et al.* [9] who studied a wire-wire configuration and proposed a preliminary wire-plates configuration as a way to increase the flowrate over the more traditional wire-wire configuration. We will see that our optimized wire-plates reference configuration provides a flow velocity of up to 8m/s and that the new proposed configuration supplies power to the fluid by decoupling the mechanism of ionization from that of acceleration and thus increases the flow velocity up to values above 10 m/s.

2. Experimental setup

In the classical wire-wire configuration studied by Berard *et al.* [8] the high electric field around the anode is responsible for both acceleration and ionization. The amount of energy deposited is limited by the appearance of a spark. To increase the velocity of the flow, one should increase the number of charged particles and/or the electric field.

SESSION 3.06, FLOW CONTROL

Our objective here is to decouple ionization and acceleration. To this end, we set the electric field at the anode close to its maximum value (i.e. just below breakdown) and we increase the acceleration of charged particles by setting a high electric field profile in the interelectrode region. To this end, we seek to make the electric field lines as parallel to the x-axis as possible. This study was performed using the finite element method-based software Comsol Multiphysics which provided 2-D simulations of the electrostatic field for various electrode configurations.

The experimental setup shown in Figure 1 is found to optimize the aforementioned design goals. The setup is comprised of a wire, two parallel cylinders and two parallel plates of 20-cm length in air at atmospheric pressure and ambient temperature. The adjustable parameters are the gap distance, the voltage, and the current. The wire is made of steel and all other electrodes of brass. The diameters of the wire and cylinders are 0.2 mm and 6 mm, respectively, and the plate cross-sectional dimensions are 8 mm × 20 mm, with rounded edges to avoid spurious breakdown.

The gap between the wire and the cylinders is adjustable from 0.3 to 4 cm. So is the gap between the cylinders and the plates. The wire electrode is raised to a positive DC potential adjustable up to 20 kV with a FUG 140-20000 power supply called the primary power supply. The cylinders are connected to ground. The plates are brought to a negative DC potential of up to -15kV with the secondary power supply. We measured the current-voltage characteristics and the flow velocities as a function of the applied potentials. The currents and voltages were obtained from the digital readouts of the power supplies. The flow velocities were measured with a glass Pitot Tube connected to a differential manometer of resolution 0.1 Pa. The distance between the Pitot tube and the plates was set to 2 mm.

The wire-plate reference configuration is obtained by removing the cylinders and grounding the plates.

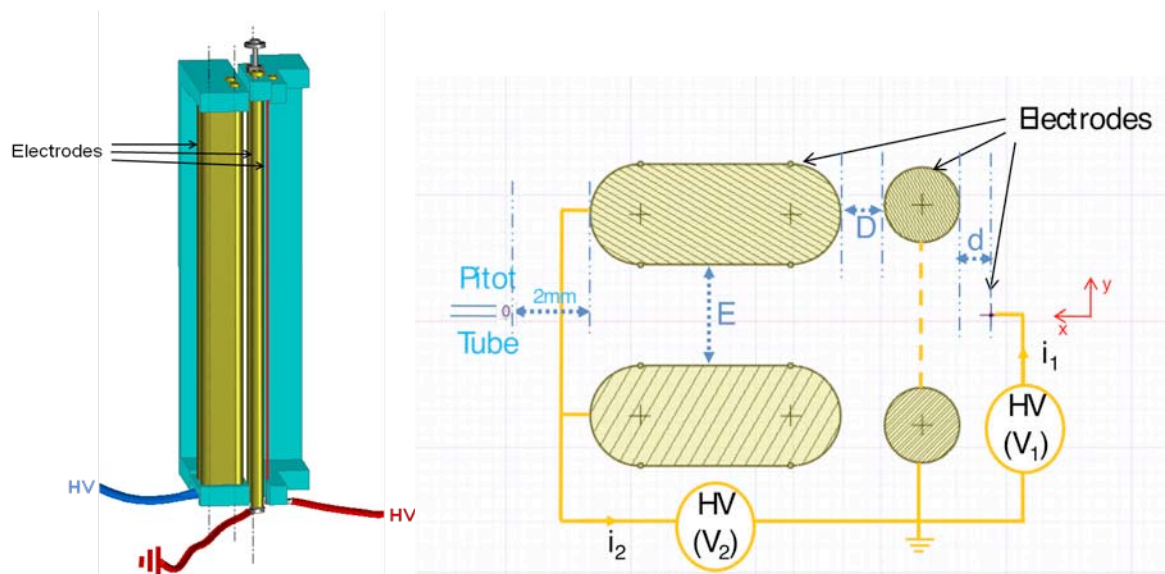


Figure 1. Experimental setup for the new wire-cylinder plate configuration showing the electrical circuit with the primary (V₁) and secondary (V₂) power supplies.

Because of the high value of the electric field around the wire (about 200 kV/cm at the wire surface), the field superimposed with the secondary power supply (maximum 6 kV/cm) did not affect the total field at the anode surface and thus did not increase the level of ionization.

Figures 2 a) and b) show that the application of V₂ creates electric field lines parallel to the x-axis, thus promoting a zone of strong acceleration between the cylinders and the plates. There are now two spatial zones with different purposes: a first zone between the wire and the cylinders where the field ionizes and provides a first acceleration of the flow and a second zone between the cylinders and the plates where only acceleration occurs. Figure 2 c) shows the component of the electric field along the x-axis, as computed with COMSOL. As can be seen from Fig. 2 c), the secondary power supply (V₂) raises the electric field in the space between the plates and the cylinders by a significant factor, thus increasing the flow speed by transferring more momentum along the x-axis to the charged particles.

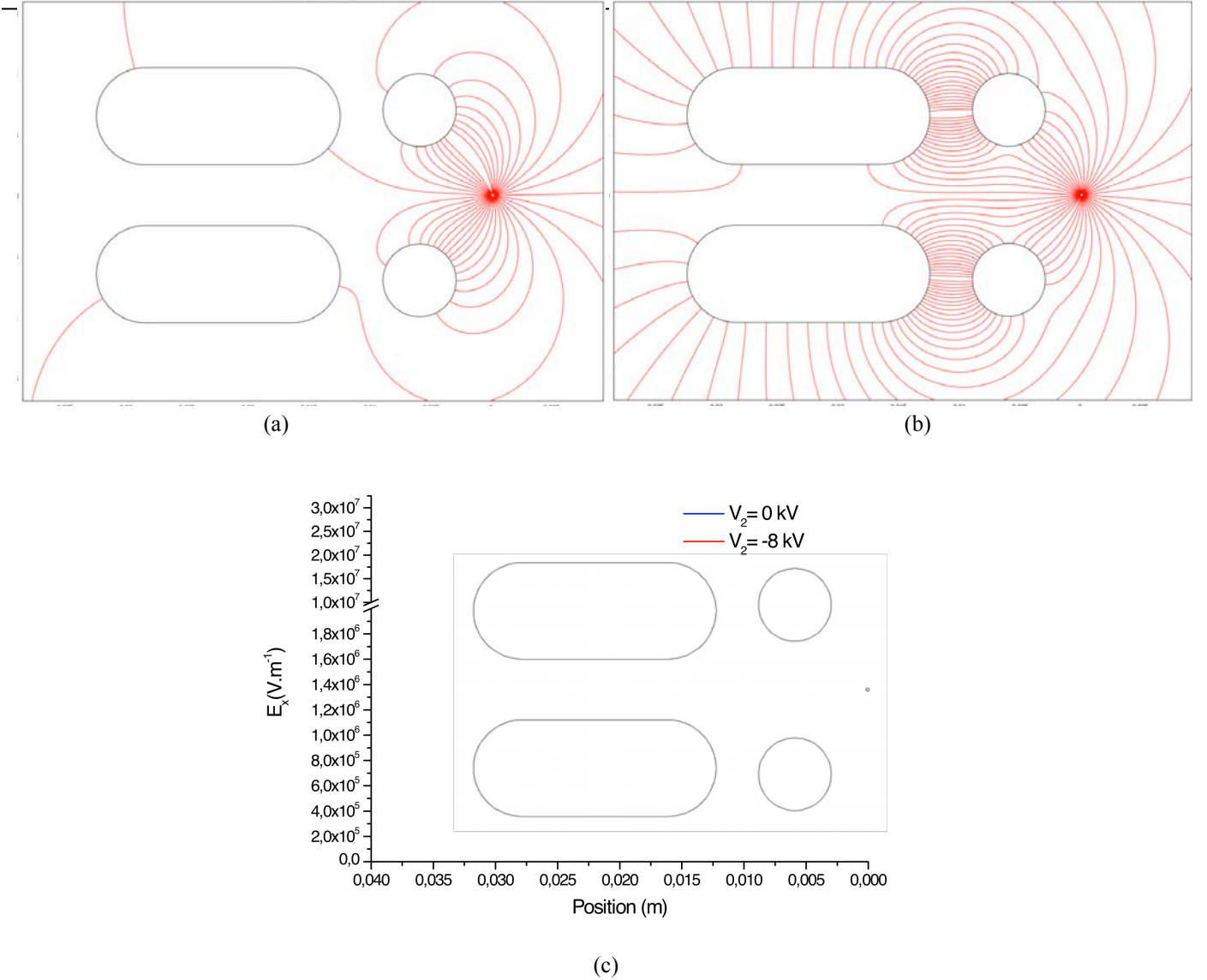


Figure 2. a) and b) Computed electric field lines for $V_2=0$ kV (a) and $V_2=-8$ kV (b). Fixed $V_1=15$ kV.
 c) Computed electric field component along the x-axis (blue: $V_2=0$ kV, red: $V_2=-8$ kV). Fixed $V_1=15$ kV.

3. Experimental results

A parametric study was conducted to maximize the ionic wind velocity as a function of the electrode gap distances and potentials. The study gave the same results as those obtained by Berard *et al.* [8], namely that the maximum current is obtained for the most compact configuration possible. However, the interelectrode gap distance should not be too small, otherwise sparks appear or the plates can become an obstacle to the flow. Thus, we chose the following optimized parameters: $E = 8$ mm, $e = 11$ mm, $D = 4$ mm and $d = 3$ mm (for definitions of these distances, see Figure 1).

We will now present the electrical and mechanical characteristics of the optimized wire-cylinder-plate setup. The optimized wire-plates configuration gives the same results as the wire-cylinder-plate with $V_2=0$ kV.

The electric power P_e transferred to the fluid can be quantified as:

$$P_e = P_1 + P_2 = V_1 \cdot i_1 + V_2 \cdot i_2,$$

where P_1 and P_2 correspond to the electric power generated by the primary and secondary power supplies. As shown in Fig. 3, the maximum potential V_1 that can be applied to the anode is independent of the potential V_2 applied to the plates. Therefore, increasing V_2 increases the power deposited into the fluid without inducing the occurrence of sparking.

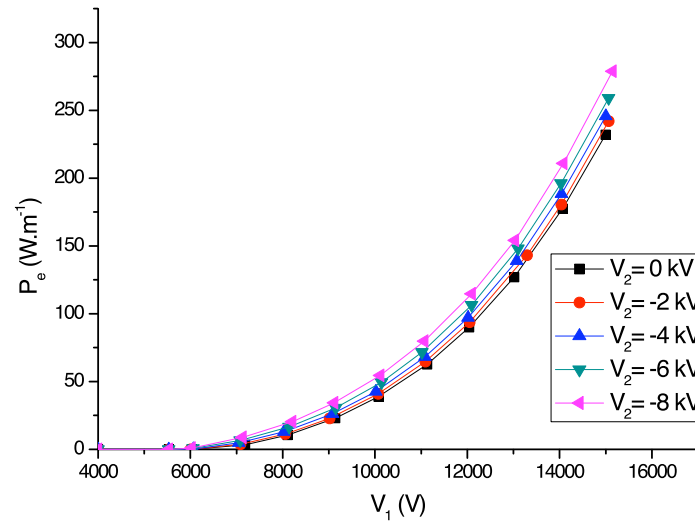
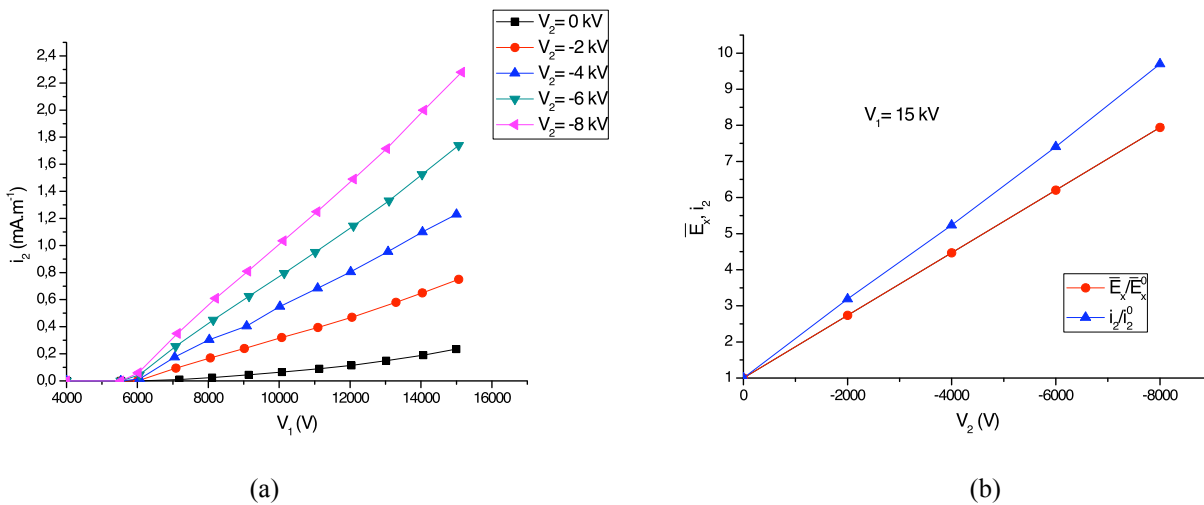


Figure 3. Electric power transferred to the fluid as a function of V_1 for different values of V_2

Figure 4a) shows that the increase of V_2 has a direct influence on i_2 , the current between the cylinders and the plates. The increase in current could be the result either of a higher acceleration of the positive ions moving towards the plates, and/or of an increase in their number density. If i_2 were related to the velocity of the positive ions that do not end up adsorbed on the plates, then it should depend linearly on the mean electrical field along the x axis. This is indeed the case, as Fig. 4b) shows a linear dependence of both the mean electrical field between the electrodes and of i_2 on V_2 . Thus, the effect of the secondary power supply is not to increase the ionization level, but rather to produce additional acceleration of the positive ions.



**Figure 4. a) Influence of V_1 on i_2 for different values of V_2 ,
b) Comparison between the influence of V_2 on the normalized mean electric field and the normalized i_2**

Figure 5 shows the flow velocity measured with the Pitot tube along the axis of the system at 2 mm downstream of the plates, as a function of the total applied electric power. For a given value of the applied electric power, we notice that the higher the potential V_2 , the higher the flow velocity even though this implies decreasing V_1 to some lower threshold value still sufficient to maintain enough ionization. Thus the electric energy is more efficiently transferred through V_2 than V_1 .

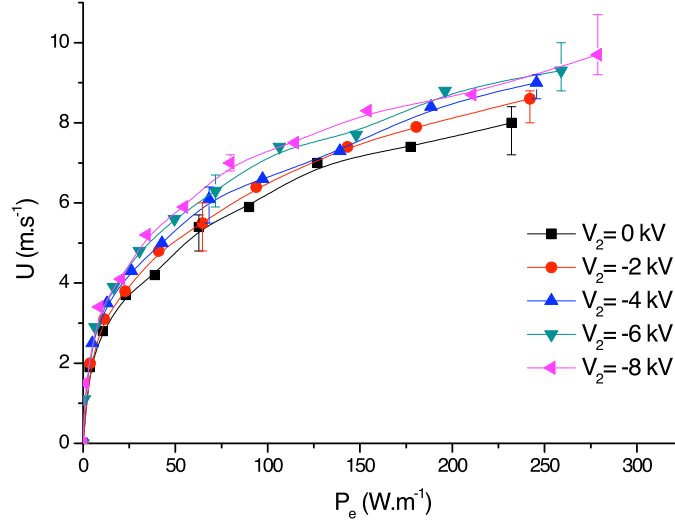


Figure 5. Flow velocity measured 2 mm downstream of the plates as a function of the applied power for various values of V_2

To quantify the benefits afforded by the new setup, we measured the velocity profiles at the exit plane of the two plates. These velocity profiles are shown in Figure 6a) for various values of V_2 . As can be seen from Figure 6a), the increase in V_2 results in an increase of both the velocity and the flow rate.

With these measurements, we can calculate the flow and mass-flow rates (D_v and D_m) through the plates and then the generated thrust using

$$T = U_{mean} \cdot D_m = \frac{\rho_{air} \cdot D_v^2}{S},$$

where h is the length of the plates (20 cm), S the exit surface area of the plates ($S=h \cdot e$), and U_{mean} the average flow velocity through S .

The thrust values, plotted in Fig. 6b), are two orders of magnitude higher than the typical values reported for DBD discharges on a flat plate (Corke *et al.* [10]). The lower thrust measured for DBD discharges on a plate or an airfoil is at least partly due to the viscous drag forces in the boundary layer of the surface where the DBD is generated (Font *et al.* [11]). Nevertheless, the thrust values obtained here are significantly higher than with these other setups, which may open new possibilities for flow control with the present geometry.

To evaluate the efficiency of the present configuration, we introduce the mechanical power transmitted to the fluid, P_m , which is equal to:

$$P_m = \iiint_V \rho_{air} U^3 d\tau = h \iint_S \rho_{air} U^3 dS,$$

We also define the efficiency of the wire-cylinders sub-system responsible for ionization and part of the acceleration:

$$\eta_1 = \frac{P_m^{V_2=0kV}}{P_1},$$

the efficiency of the cylinders-plates sub-system that provides secondary acceleration:

$$\eta_2 = \frac{P_m^{V_2} - P_m^{V_2=0kV}}{P_2},$$

and finally the efficiency of the overall system:

$$\eta = \frac{P_m}{P_e}.$$

Figure 6c) shows that a 16% increase (from 175 to 210 W) of the total applied electric power through the increase of V_2 (i.e. P_2) leads to a 77% increase in the mechanical power. Thus the secondary power supply is particularly efficient in increasing the acceleration of the flow.

We can now quantify the efficiencies of both power supplies. The value of η_2 is 15.5%, whereas the value of η_1 is only 0.7%.

The overall efficiency rises from 0.7% ($V_2 = 0$ kV) to 1.1% ($V_2 = -8$ kV). Since V_2 is responsible only for acceleration and V_1 for both acceleration and ionization, the difference between η_1 and η_2 may come from either a low efficiency of the ionization process or/and a higher efficiency of the acceleration produced by V_2 than by V_1 .

Regarding the ionization efficiency, it is well known that most of the energy around the anode serves to excite the vibrational and electronic states of molecular species, in particular molecular nitrogen (Raizer *et al.* [12]), rather than to ionize. Thus the ionization efficiency is expected to be small.

Regarding the acceleration efficiencies, we can see from Figures 2a) and b) that the electric field created by V_1 (between the wire and the cylinders) is mostly non parallel to the x-axis. This represents a loss of energy since the macroscopic flow is directed along the x-axis. In contrast, the electric field created by V_2 i.e. the “second acceleration zone” between the cylinders and the plates has been shaped to be as parallel to the x-axis as possible. Thus the acceleration promoted by V_2 is expected to be more efficient than the acceleration promoted by V_1 .

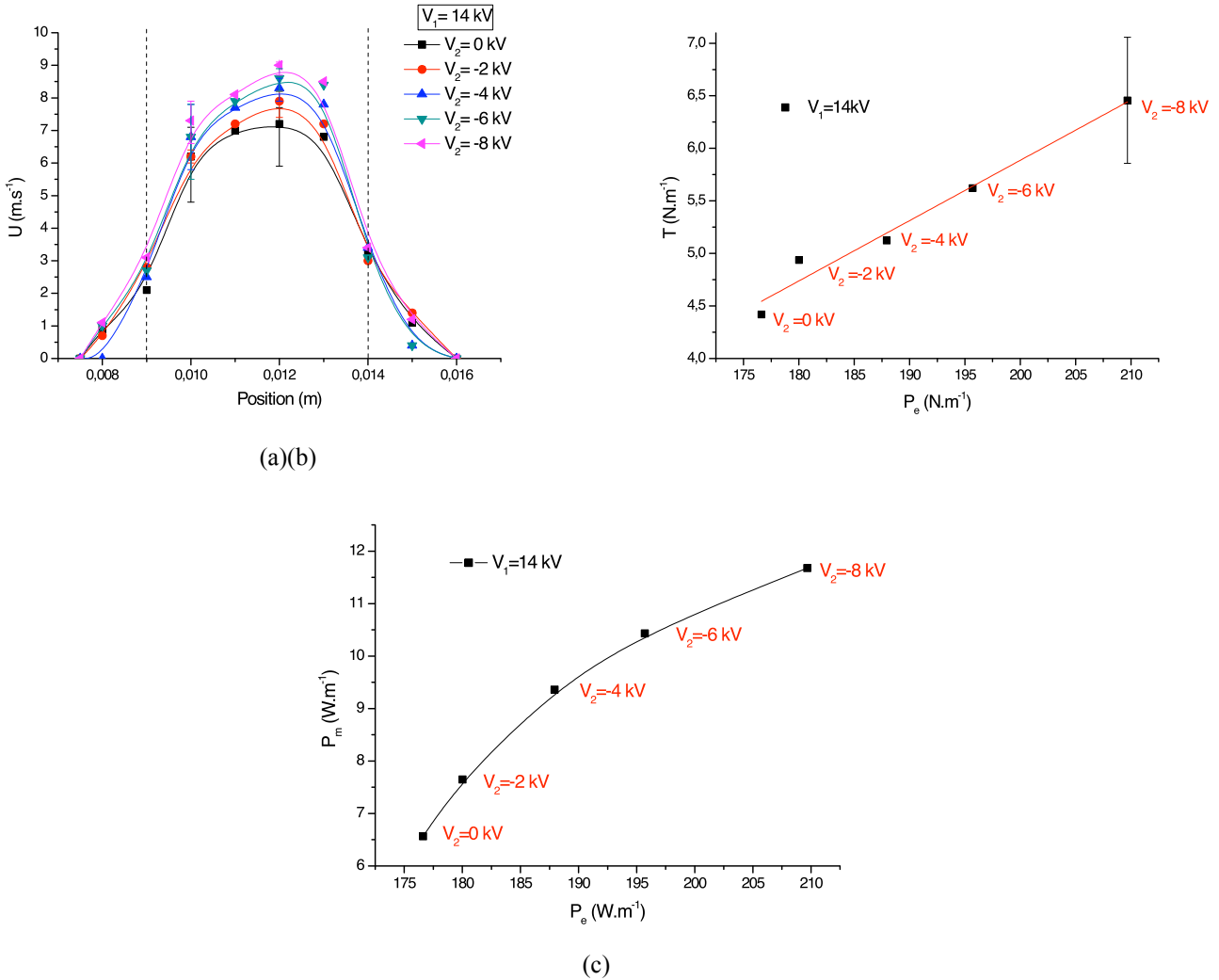


**Figure 6. a) Lateral flow velocity profile 2 mm downstream of the plates (the dashes represent the position of the plates)
 b) Thrust as a function of the electrical power for varying V_2
 c) Mechanical power as a function of the electrical power for varying V_2**

3. Conclusions

In this paper, we have presented a wire-plates reference configuration that we have optimized to generate high flow velocities up to $8 \text{ m}\cdot\text{s}^{-1}$, a flow rate per unit electrode length of up to $0.17 \text{ m}^2\cdot\text{s}^{-1}$, and a thrust per unit electrode length of up to $4.5 \text{ N}\cdot\text{m}^{-1}$. This value of the thrust is almost two orders of magnitude higher than the highest values of thrust obtained with DBDs on airfoils.

We then proposed a novel wire-cylinders-plates configuration that further increases the ionic wind velocity by decoupling the mechanism of acceleration from that of ionization. With this new configuration, two main results are obtained. First, we are able to deposit more energy to accelerate the flow without changing the ionization process. This provides an increased flow velocity of up to $10 \text{ m}\cdot\text{s}^{-1}$, flow rate and thrust generated by unit electrode length of up to $0.2 \text{ m}^2/\text{s}$ and $6.5 \text{ N}/\text{m}$, respectively. This value of the thrust is 45% higher than for the reference configuration. Second, the efficiency of the acceleration process being much higher

than the efficiency of ionization, the overall efficiency of the new configuration increases significantly. The 45% increase in thrust is obtained by increasing the electric power by only 16%.

To obtain higher velocities, one possible improvement would be to increase the efficiency of the ionization process. This is currently investigated through the use of nanosecond repetitively pulsed discharges as explained in Lacoste *et al.* [9] and as already used by Opaits *et al.* [3] for DBD discharges.

In parallel, a numerical code is being developed to solve the Navier-Stokes equations coupled to Poisson's equation, incorporating a detailed kinetic mechanism extracted from Kossyi *et al.* [13]. The results are expected to increase our understanding of the chemical kinetics and to provide a reduced model limited to the main species responsible for momentum transfer in order to conduct further optimization studies.

Acknowledgments

The authors would like to thank Philippe Bérard for useful discussions, Denis Packan (ONERA) for lending one of the power supplies, Eric Moreau (LEA) for help with the design of the glass Pitot tube, and Alain Walton and Erika Jean-Bart for help constructing the setup.

References

- [1] Forte M., Jolibois J., Moreau E. and Touchard G., "Optimization of a Dielectric Barrier Discharge Actuator by Stationary and Non-stationary Measurements of the induced Flow velocity – Application to Airflow control". AIAA paper 2006-286, *3rd Flow Control Conference*, San Francisco, California, June 2006.
- [2] Corke T. C., Mertz B., and Patel M.P., "Plasma flow control optimized airfoil". AIAA paper 2006-1208, *44th AIAA Aerospace Sciences Meeting & Exhibit*, Reno, Nevada, January 2006.
- [3] Opaits D.F., Likhanskii A.V., Neretti G., Zaidi S., Schneider M.N., Miles R.B., Macheret S.O., "Experimental investigation of dielectric barrier discharge plasma actuators driven by repetitive high-voltage nanosecond pulses with dc or low frequency sinusoidal bias". *Journal of Applied Physics*, 104:04334, 2008.
- [4] Corke T. C., Post M. L. and Orlov D. M., "Sdbd plasma enhanced aerodynamics: concepts, optimization and applications". *Progress in Aerospace Sciences*, 43:193–217, 2007.
- [5] Moreau E., Sosa R. and Artana G., "Electric wind produced by surface plasma actuators: a new dielectric barrier discharge based on a three-electrode geometry". *Journal of Physics D, Applied Physics*, 41: 115204, 2008.
- [6] Boeuf J. P., Lagmich Y., Callegari T. and Pitchford L. C., "Electrohydrodynamic force and acceleration in surface discharges". AIAA paper 2006-3574, *37th AIAA Plasmadynamics and Lasers Conference*, San Francisco, California, June 2006.
- [7] Matteo-Velez J-C, Degond P, Rogier F, Seraudie A. and Thivet F., "Modelling wire-to-wire corona discharge action on aerodynamics and comparison with experiment". *Journal of Physics D, Applied Physics*, 41: 035205, 2008.
- [8] Bérard P., Lacoste D. A. and Laux C. O., "Measurements and Simulations of the Ionic Wind Produced by a DC Corona Discharge in Air, Helium and Argon". AIAA paper 2006-4611, *38th AIAA Plasmadynamics and Lasers Conference*, Miami, Florida, June 2007.
- [9] Lacoste D. A., Pai D. Z., Laux C. O., "Ion wind effect in a positive DC corona discharge in atmospheric pressure air". AIAA paper 2004-0354, *42nd Aerospace Sciences Meeting & Exhibit*, Reno, Nevada, January 2004.
- [10] Corke T. C., Post M. L. and Orlov D. M., "Single dielectric barrier discharge plasma enhanced aerodynamics: physics, modeling and applications". *Experiments in Fluids*, 46:1-26, 2009.
- [11] Font G. I., Enloe C. L. and McLaughlin T. E., "Effect of Volumetric Momentum Addition on the Total Force Production of a Plasma Actuator". AIAA paper 2009-4285, *39th Fluid Dynamics Conference*, San Antonio, Texas, June 2009.
- [12] Raizer Y.P. Gas Discharge Physics. In *Springer*, 1997.
- [13] Kossyi I. A., Kostinsky A. Yu., Matveyev A. A. and Silakov V. P., "Kinetic scheme of the non-equilibrium discharge in nitrogen-oxygen mixtures". *Plasma Sources Sci. Technol.*, 1: 207-220, 1992.